Phase loops in density-functional-theory calculations of adsorption in nanoscale pores

G. L. Aranovich and M. D. Donohue
Department of Chemical Engineering, The Johns Hopkins University, Baltimore, Maryland 21218
(Received 10 May 1999)

Phase loops with multiple solutions are observed in calculations of lattice density-functional theory. It is shown that the standard numerical methods for solving such problems distort the solution. A technique is proposed to obtain multiple solutions for phase equilibria in confined fluids. This method gives the entire phase equilibrium curve, including hidden points which determine wetting transitions and capillary condensation. A synergetic effect of walls on adsorption in nanoscale pores is analyzed. [S1063-651X(99)14711-1]

PACS number(s): 68.10.Jy, 71.15.Mb

INTRODUCTION

The physics of fluids in micropores has been studied extensively [1–7]. The combination of intermolecular and molecule-wall interactions results in differences between fluids in pores and bulk fluids [8]. These differences include wetting phase transitions [9], capillary condensation [10], liquid-liquid phase separation [11], adsorption hysteresis [12], and pore-pore correlation effects [13].

Density-functional theory (DFT) [14,15] is one of the most efficient tools to study the behavior of confined fluids. DFT considers the intrinsic Helmholtz free energy F as a functional, $F[\rho(\mathbf{r})]$, of the density distribution, $\rho(\mathbf{r})$ [14]. At equilibrium, the grand potential Ω [15] is minimized to give the equation for the equilibrium density profile [16]:

$$\frac{\delta\Omega[\rho(\mathbf{r})]}{\delta\rho(\mathbf{r})}=0. \tag{1}$$

There are two difficulties in DFT: to define a model for $F[\rho(\mathbf{r})]$ and to solve the equation of equilibrium. Defining a model for $F[\rho(\mathbf{r})]$ requires both assumptions and simplifications. These include idealized potential functions, pairwise additivity, mean-field assumptions, and assumptions about the equation of state for fluid in the bulk. However, even with these assumptions, minimization of Ω results in a complex integrodifferential equation [14,15] which is not solvable analytically. Finding a numerical solution for the equilibrium equation is straightforward if the equation does not have multiple solutions. However, the most interesting phenomena occur when there are multiple solutions. This includes wetting phase transitions, capillary condensation, and hysteresis. Since the standard numerical methods, such as successive substitutions and the Newton-Raphson procedure [17], fail when there are multiple solutions, this can result in a loss of important information or in distortion of the solution. However, though the method of iterations is used widely in DFT approaches [14,15,18], this problem has never been analyzed in detail. In this paper, we examine this problem using a simple example—DFT applied to a confined lattice. We also demonstrate a numerical algorithm which can solve simultaneously multiple equations with multiple solutions. Using this algorithm, we analyze the synergism of two walls on adsorption of a fluid in nanoscale pores. This analysis shows both a wetting phase transition and capillary condensation.

Here, we present an analysis of adsorption behavior in slitlike pores using density-functional theory for a confined lattice. This grid-based (or real space) DFT [18] has the free energy as a functional of the density distribution, $\rho(i,j,k)$, on lattice sites, (i,j,k). For a slit pore between two planes, the three-dimensional density distribution can be reduced to a one-dimensional density distribution, $\rho(i)$. To write the free-energy functional, we follow the derivation of Ono and Kondo [19]. This approach has been used to describe density gradients at vapor-liquid [20], liquid-solid [21], and vapor-solid [22] interfaces. Fluid-solid interfaces have been considered for semi-infinite cases (adsorption in macropores) and for adsorption in slit pores at temperatures above the vapor-liquid critical point. However, the effect of wall synergism on confined fluids in nanoscale pores has not been analyzed.

DENSITY-FUNCTIONAL THEORY FOR A CONFINED LATTICE

Consider a binary mixture of A and B molecules on a lattice with two boundaries (walls). Each site of the lattice can contain an A molecule or a B molecule. There are interactions between nearest neighbors with ε_{AA}, ε_{AB}, ε_{BB} being the energies for adsorbate-adsorbate interactions, and ε_{AS}, ε_{BS} being the energies for adsorbate-surface interactions. One of the components (say B) can be holes, and, therefore, a one-component system is a particular case with ε_{AB}, ε_{BB}, and ε_{BS} being zero.

We assume the lattice fluid is in contact with a flat surface at the planes of $i=0$ (the first layer of adsorbed molecules is in the plane of $i=1$) and $i=N+1$ (the last layer of adsorbed molecules is in the plane of $i=N$). In the mean-field approximation, the energy of interaction, $E(i,i+1)$, between molecules on two neighboring sites in neighboring layers, is

$$E(i,i+1)=\varepsilon_{AA}\rho_A(i)\rho_A(i+1)+\varepsilon_{AB}\rho_B(i)\rho_A(i+1)+\varepsilon_{AB}\rho_A(i)\rho_B(i+1)+\varepsilon_{BB}\rho_B(i)\rho_B(i+1). \tag{2}$$

For neighboring sites in the same layer

$$E(i,i)=\varepsilon_{AA}\rho_A^2(i)+2\varepsilon_{AB}\rho_B(i)\rho_A(i)+\varepsilon_{BB}\rho_B^2(i), \quad (3)$$

where $\rho_A(i)$ is the mole fraction of A molecules in the ith layer; the mole fraction of B molecules in the ith layer, $\rho_B(i)$, is $1-\rho_A(i)$. Therefore, the Hamiltonian H for the lattice fluid between two walls can be written in the following form:

$$\begin{aligned}H=(1/2)\sum_{i=2}^{N-1}&[z_1\rho_A(i)\rho_A(i+1)\varepsilon_{AA}+z_1\rho_A(i)\rho_A(i-1)\varepsilon_{AA}+z_1\rho_B(i)\rho_B(i+1)\varepsilon_{BB}+z_1\rho_B(i)\rho_B(i-1)\varepsilon_{BB}\\&+z_1\rho_A(i)\rho_B(i+1)\varepsilon_{AB}+z_1\rho_A(i+1)\rho_B(i)\varepsilon_{AB}+z_1\rho_A(i)\rho_B(i-1)\varepsilon_{AB}+z_1\rho_A(i-1)\rho_B(i)\varepsilon_{AB}+z_2\rho_A(i)^2\varepsilon_{AA}\\&+z_2\rho_B(i)^2\varepsilon_{BB}+2z_2\rho_A(i)\rho_B(i)\varepsilon_{AB}]+\rho_A(1)\varepsilon_{AS}+\rho_B(1)\varepsilon_{BS}+\rho_A(N)\varepsilon_{AS}+\rho_B(N)\varepsilon_{BS}+(1/2)[z_1\rho_A(1)\rho_A(2)\varepsilon_{AA}\\&+z_1\rho_B(1)\rho_B(2)\varepsilon_{BB}+z_1\rho_A(1)\rho_B(2)\varepsilon_{AB}+z_1\rho_A(2)\rho_B(1)\varepsilon_{AB}+z_1\rho_A(N-1)\rho_A(N)\varepsilon_{AA}+z_1\rho_B(N-1)\rho_B(N)\varepsilon_{BB}\\&+z_1\rho_A(N-1)\rho_B(N)\varepsilon_{AB}+z_1\rho_A(N)\rho_B(N-1)\varepsilon_{AB}]. \quad (4)\end{aligned}$$

Here z_2 is the monolayer coordination number, and z_1 is the number of bonds for a molecule in some layer with molecules in a neighboring layer; $z_1=(z_0-z_2)/2$, where z_0 is the coordination number of the three-dimensional lattice. Note that the assumption given by Eqs. (2) and (3) is equivalent to the mean-field approximation in Ono and Kondo theory [19,20].

The entropy of the system in the mean-field approximation can be written in the form [19,20]:

$$S=-k_B\sum_{i=1}^{N}\{\rho_A(i)\ln[\rho_A(i)]+\rho_B(i)\ln[\rho_B(i)]\}, \quad (5)$$

where k_B is Boltzmann's constant. From Eqs. (4) and (5), it follows that the free energy F is

$$\begin{aligned}F=(1/2)\sum_{i=2}^{N-1}&[z_l\rho_A(i)\rho_A(i+1)\varepsilon_{AA}+z_1\rho_A(i)\rho_A(i-1)\varepsilon_{AA}+z_1\rho_B(i)\rho_B(i+1)\varepsilon_{BB}+z_1\rho_B(i)\rho_B(i-1)\varepsilon_{BB}+z_1\rho_A(i)\rho_B(i\\&+1)\varepsilon_{AB}+z_1\rho_A(i+1)\rho_B(i)\varepsilon_{AB}+z_1\rho_A(i)\rho_B(i-1)\varepsilon_{AB}+z_1\rho_A(i-1)\rho_B(i)\varepsilon_{AB}+z_2\rho_A(i)^2\varepsilon_{AA}+z_2\rho_B(i)^2\varepsilon_{BB}\\&+2z_2\rho_A(i)\rho_B(i)\varepsilon_{AB}]+\rho_A(1)\varepsilon_{AS}+\rho_B(1)\varepsilon_{BS}+\rho_A(N)\varepsilon_{AS}+\rho_B(N)\varepsilon_{BS}+(1/2)[z_1\rho_A(1)\rho_A(2)\varepsilon_{AA}+z_1\rho_B(1)\rho_B(2)\varepsilon_{BB}\\&+z_1\rho_A(1)\rho_B(2)\varepsilon_{AB}+z_1\rho_A(2)\rho_B(1)\varepsilon_{AB}+z_1\rho_A(N-1)\rho_A(N)\varepsilon_{AA}+z_1\rho_B(N-1)\rho_B(N)\varepsilon_{BB}+z_1\rho_A(N-1)\rho_B(N)\varepsilon_{AB}\\&+z_1\rho_A(N)\rho_B(N-1)\varepsilon_{AB}]+k_BT\sum_{i=1}^{N}\{\rho_A(i)\ln[\rho_A(i)]+\rho_B(i)\ln[\rho_B(i)]\}, \quad (6)\end{aligned}$$

where T is the absolute temperature.

Values of $\rho_A(i)$ must be found that minimize F under the constraint

$$N_s\sum_{i=1}^{N}\rho_A(i)=N_A, \quad (7)$$

where N_s is the total number of sites in the lattice, and N_A is the total number of A molecules in the system. This problem can be solved using the standard method of Lagrange's multipliers [23] by considering a function:

$$\begin{aligned}\Omega'[\rho_A(1),\rho_A(2)\cdots\rho_A(N)]&=F[\rho_A(1),\rho_A(2)\cdots\rho_A(N)]\\&\quad-\mu^*\left\{\sum_{i=1}^{N}[\rho_A(i)-N_A/N_s]\right\}, \quad (8)\end{aligned}$$

which gives the following equations for the Lagrange's multiplier μ^*:

$$\partial\Omega'/\partial\rho_A(i)=0. \quad (9)$$

Note that Eq. (9) is the lattice analog of Eq. (1).

Substituting Eq. (6) into Eq. (8) and then into Eq. (9), and taking into account that $\rho_B(i)=1-\rho_A(i)$, we obtain for $2\leqslant i\leqslant N-1$:

$$\begin{aligned}\mu^*=&-z_1\rho_A(i+1)\Delta-z_1\rho_A(i-1)\Delta-z_2\rho_A(i)\Delta\\&+z_0(\varepsilon_{AB}-\varepsilon_{BB})+kT\ln\{\rho_A(i)/[1-\rho_A(i)]\}, \quad (10)\end{aligned}$$

where $\Delta=2\varepsilon_{AB}-\varepsilon_{AA}-\varepsilon_{BB}$.

Since the layers between the two walls are in equilibrium with the bulk, Eq. (10) has to be valid for the bulk with $\rho_A(i+1)=\rho_A(i-1)=\rho_A(i)=\rho_A$ where ρ_A is the mole fraction of A molecules in the bulk. This gives from Eq. (10):

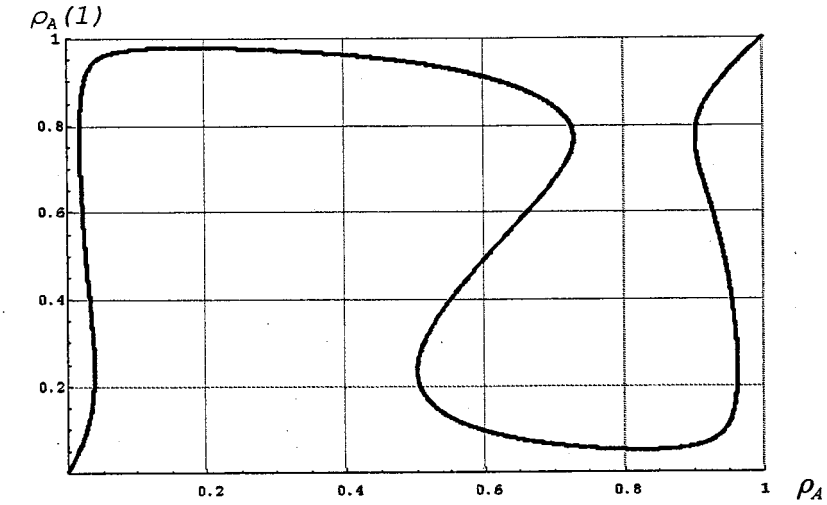

FIG. 1. Composition of fluid in a slitlike pore as a function of ρ_A for $N=2$, $\varepsilon_{AA}/kT=-1.4$, $\varepsilon_{AS}/kT=-1.0$, and $\varepsilon_{AB}/kT=\varepsilon_{BB}/kT=\varepsilon_{BS}/kT=0$.

$$\mu^*=-z_0\rho_A\Delta+z_0(\varepsilon_{AB}-\varepsilon_{BB})+kT\ln[\rho_A/(1-\rho_A)]. \tag{11}$$

Combining Eqs. (10) and (11), we obtain for $2\leqslant i\leqslant N-1$:

$$\ln\frac{\rho_A(i)(1-\rho_A)}{[1-\rho_A(i)]\rho_A}-\{z_1[\rho_A(i+1)-\rho_A]+z_2[\rho_A(i)-\rho_A] +z_1[\rho_A(i-1)-\rho_A]\}\Delta/kT=0. \tag{12}$$

For $i=1$, instead of Eq. (12), Eqs. (8) and (9) give

$$\ln\frac{\rho_A(1)(1-\rho_A)}{[1-\rho_A(i)]\rho_A}-\{z_2[\rho_A(1)-\rho_A] +z_1[\rho_A(2)-\rho_A]-z_1\rho_A\}\Delta/kT-z_1(\varepsilon_{AB}-\varepsilon_{BB})/kT +(\varepsilon_{AS}-\varepsilon_{BS})/kT=0. \tag{13}$$

Since we consider the walls to be identical, there is a condition of symmetry:

$$\rho_A(1)=\rho_A(N). \tag{14}$$

Equation (12) is a set of nonlinear finite difference equations of second order. They relate the composition in each layer to the compositions in the neighboring layers. Equations (13) and (14) are boundary conditions for Eq. (12). Together, they determine a self-sufficient set of N equations with respect to N unknowns, $\rho_A(1),\rho_A(2)\cdots\rho_A(N)$. Equation (12) has been considered in the Ono-Kondo theory for semi-infinite adsorbate [19–21]. However, it has not been analyzed for a fluid in a slitlike pore at temperatures below the vapor-liquid critical point. For low temperatures, there is a synergetic effect between the walls, and the system behaves differently from a semi-infinite system. In particular, while a semi-infinite system can have steps in the adsorption isotherm [22], it cannot exhibit the nanoscale ''capillary condensation'' discussed here.

NEW TECHNIQUE FOR EQUATIONS WITH MULTIPLE SOLUTIONS

In the set of Eqs. (12)–(14), each equation can have multiple roots, and this complicates finding the global free energy minimum. However, these multiple roots determine the behavior in the pore and cannot be ignored. There are a number of standard methods to solve nonlinear equations. In particular, the Newton-Raphson procedure, the method of successive substitutions, the method of Wegstein, and others are used widely in practice [17]. However, these standard methods do not work when a nonlinear equation has multiple

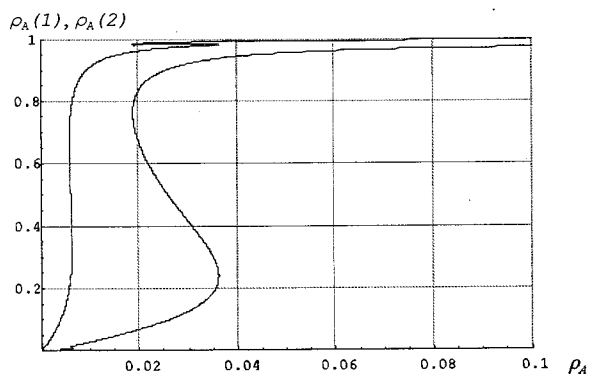

FIG. 2. Composition of the first and second layers in a slitlike pore as a function of ρ_A for $N=4$, $\varepsilon_{AA}/kT=-1.1$, $\varepsilon_{AS}/kT=-3.0$, and $\varepsilon_{AB}/kT=\varepsilon_{BB}/kT=\varepsilon_{BS}/kT=0$.

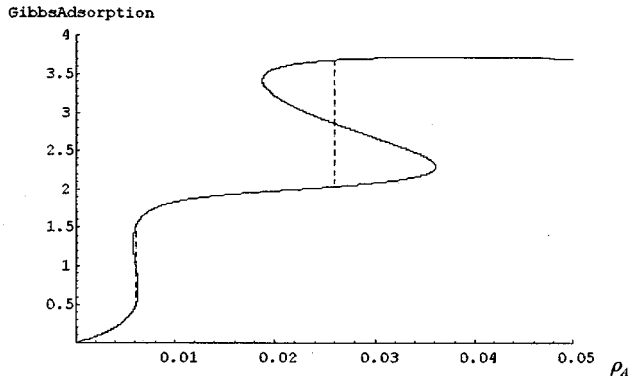

FIG. 3. Isotherm of the Gibbs adsorption in a slitlike pore at $N=4$, $\varepsilon_{AA}/kT=-1.1$, $\varepsilon_{AS}/kT=-3.0$, and $\varepsilon_{AB}/kT=\varepsilon_{BB}/kT=\varepsilon_{BS}/kT=0$.

roots. In [24], we proposed a new numerical algorithm for such problems. This algorithm is based on taking the derivative of the density distribution with respect to one of the parameters and then integrating the differential equation numerically. We have demonstrated that this algorithm is accurate for calculating compositions in adsorption monolayers for multiphase systems. However, in Ref. [24], we considered only one nonlinear equation with one unknown. In order to analyze Eqs. (12)–(14), it is necessary to generalize this method for sets of nonlinear equations. Since this generalization is not trivial, it is discussed here.

Taking the derivative from the left side terms of Eq. (12) with respect to ρ_A gives

$$-\frac{z_1\Delta}{kT}\frac{\partial\rho_A(i+1)}{\partial\rho_A}+\left\{\frac{1}{\rho_A(i)[1-\rho_A(i)]}-\frac{z_2\Delta}{kT}\right\}\frac{\partial\rho_A(i)}{\partial\rho_A}-\frac{z_1\Delta}{kT}\frac{\partial\rho_A(i-1)}{\partial\rho_A}=\frac{1}{\rho_A(1-\rho_A)}-\frac{z_0\Delta}{kT}. \tag{15}$$

The same manipulation with Eq. (13) results in the following equation:

$$-\frac{z_1\Delta}{kT}\frac{\partial\rho_A(2)}{\partial\rho_A}+\left\{\frac{1}{\rho_A(1)[1-\rho_A(1)]}-\frac{z_2\Delta}{kT}\right\}\frac{\partial\rho_A(1)}{\partial\rho_A}=\frac{1}{\rho_A(1-\rho_A)}-\frac{z_0\Delta}{kT}. \tag{16}$$

Equations (15) and (16) are linear with respect to derivatives $\partial\rho_A(i)/\partial\rho_A$. They can be represented in the following matrix form:

$$\mathbf{M}_0\mathbf{D}_0=\mathbf{B}_0, \tag{17}$$

where $\mathbf{B}_0$ and $\mathbf{D}_0$ are N-component vectors:

$$\mathbf{B}_0=\begin{Bmatrix}\frac{1}{\rho_A(1-\rho_A)}-\frac{z_0\Delta}{kT}\\ \frac{1}{\rho_A(1-\rho_A)}-\frac{z_0\Delta}{kT}\\ \cdots\\ \frac{1}{\rho_A(1-\rho_A)}-\frac{z_0\Delta}{kT}\end{Bmatrix}, \tag{18}$$

$$\mathbf{D}_0=\begin{Bmatrix}\partial\rho_A(1)/\partial\rho_A\\ \partial\rho_A(2)/\partial\rho_A\\ \cdots\\ \partial\rho_A(N)/\partial\rho_A\end{Bmatrix}, \tag{19}$$

and $\mathbf{M}_0$ is $N\times N$ matrix:

$$\mathbf{M}_0=\begin{pmatrix} a_1 & -\frac{z_1\Delta}{kT} & 0 & \cdots & 0 & 0 & 0\\ -\frac{z_1\Delta}{kT} & a_2 & -\frac{z_1\Delta}{kT} & \cdots & 0 & 0 & 0\\ 0 & -\frac{z_1\Delta}{kT} & a_3 & \cdots & 0 & 0 & 0\\ \cdots & \cdots & \cdots & \cdots & \cdots & \cdots & \cdots\\ 0 & 0 & 0 & \cdots & a_{N-2} & -\frac{z_1\Delta}{kT} & 0\\ 0 & 0 & 0 & \cdots & -\frac{z_1\Delta}{kT} & a_{N-1} & -\frac{z_1\Delta}{kT}\\ 0 & 0 & 0 & \cdots & 0 & -\frac{z_1\Delta}{kT} & a_N \end{pmatrix}, \tag{20}$$

where $a_i=1/\rho_A(i)[1-\rho_A(i)]-z_2\Delta/kT$ for $1\leqslant i\leqslant N$.

The solution of Eq. (17) can be represented in the following form:

$$\partial\rho_A(i)/\partial\rho_A=\det[\mathbf{M}_i]/\det[\mathbf{M}_0]. \tag{21}$$

Here $\mathbf{M}_i$ is the matrix defined by Eq. (20) where ith column is substituted by vector $\mathbf{B}_0$, $1\leqslant i\leqslant N$, and ''det'' is the determinant symbol.

Since the problem is symmetric, in the numerical analysis we consider only the first n layers where $n=N/2$ for even N and $n=(N+1)/2$ for odd N. For $i=1$, in the limit of small concentrations, Eq. (13) gives

$$\rho_A(1)=\rho_A\exp[(\varepsilon_{BS}-\varepsilon_{AS})/kT+z_1(\varepsilon_{AB}-\varepsilon_{BB})/kT]. \tag{22}$$

From Eq. (12), in the limit of small concentrations, we get

$$\rho_A(i)=\rho_A \tag{23}$$

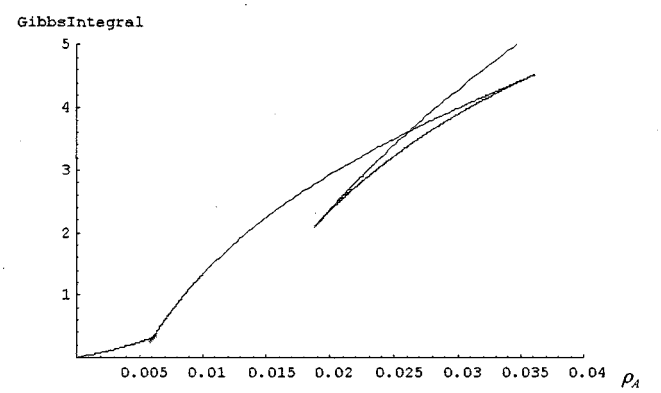

FIG. 4. Gibbs integral as a function of ρ_A for a slitlike pore at $N=4$, $\varepsilon_{AA}/kT=-1.1$, $\varepsilon_{AS}/kT=-3.0$, and $\varepsilon_{AB}/kT=\varepsilon_{BB}/kT=\varepsilon_{BS}/kT=0$. There are two points of self-intersection where $\rho_A\approx 0.006$ and $\rho_A\approx 0.026$. These points are indicated in Fig. 3 by dashed lines.

for $2\leqslant i\leqslant n$.

Calculation of the unknown values of $\rho_A(1),\rho_A(2)\ldots\rho_A(n)$ as functions of ρ_A was performed from $\rho_A=0$ to $\rho_A=1$ with a small stepsize, δ (typically 0.001–0.0005). For $\rho_A=0$, all $\rho_A(i)$ are zeros. For $\rho_A=\delta$, we have

$$\rho_A(1)=\delta\exp[(\varepsilon_{BS}-\varepsilon_{AS})/kT+z_1(\varepsilon_{AB}-\varepsilon_{BB})/kT] \tag{24}$$

and

$$\rho_A(i)=\delta \tag{25}$$

for $2\leqslant i\leqslant n$.

Equations (24) and (25) give the first step of calculation. All further calculations are based on Eq. (21). If the absolute values of derivatives $\partial\rho_A(i)/\partial\rho_A$ are not large (say, each of them less than some value α), then each next step is calculated from the previous step using the following equations:

$$\rho_A^{k+1}=\rho_A^k+\delta, \tag{26}$$

$$\rho_A^{k+1}(i)=\rho_A^k(i)+\frac{\partial\rho_A^k(i)}{\partial\rho_A}\,\delta, \tag{27}$$

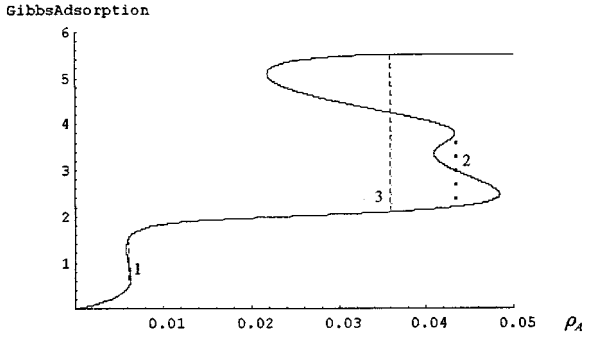

FIG. 5. Isotherm of the Gibbs adsorption in a slitlike pore at $N=6$, $\varepsilon_{AA}/kT=-1.1$, $\varepsilon_{AS}/kT=-3.0$, and $\varepsilon_{AB}/kT=\varepsilon_{BB}/kT=\varepsilon_{BS}/kT=0$.

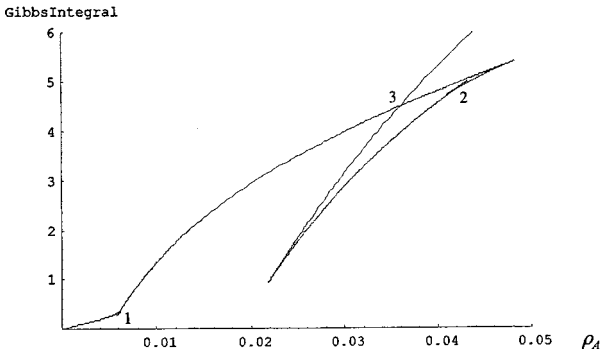

FIG. 6. Gibbs integral as a function of ρ_A for a slitlike pore at $N=6$, $\varepsilon_{AA}/kT=-1.1$, $\varepsilon_{AS}/kT=-3.0$, and $\varepsilon_{AB}/kT=\varepsilon_{BB}/kT=\varepsilon_{BS}/kT=0$. There are three points of self-intersection where $\rho_A\approx 0.006$, $\rho_A\approx 0.036$, and $\rho_A\approx 0.042$. The last one is almost invisible at this scale—therefore, the fragment of this graph is given in Fig. 7 at smaller scale.

where $k+1$ is the next step, and k characterizes the previous step. Having $\rho_A^{k+1}(i)$ from Eq. (27), one can calculate $\partial\rho_A^{k+1}(i)/\partial\rho_A$ from Eq. (21), etc. So, Eqs. (26) and (27) give $\rho_A(i)$ as functions of ρ_A by numerical integration of the derivatives, $\partial\rho_A(i)/\partial\rho_A$, given by Eq. (21).

If any of the derivatives, $\partial\rho_A(i)/\partial\rho_A$, becomes greater than α at some step of calculation (say, greater than unity), the variable of integration is switched. This requires two procedures. The first is a search for the derivative with the maximum absolute value: say, $\partial\rho_A^k(m)/\partial\rho_A$ is greater or equal than all other values of $\partial\rho_A^k(i)/\partial\rho_A$. The second is using the following equations:

$$\rho_A^{k+1}(m)=\rho_A^k(m)+\delta, \tag{28}$$

$$\rho_A^{k+1}(i)=\rho_A^k(i)+\frac{\partial\rho_A^k(i)/\partial\rho_A}{\partial\rho_A^k(m)/\partial\rho_A}\,\delta, \tag{29}$$

$$\rho_A^{k+1}=\rho_A^k+\frac{1}{\partial\rho_A^k(m)/\partial\rho_A}\,\delta, \tag{30}$$

instead of Eqs. (26) and (27).

The procedure given by Eqs. (24)–(30) allows one to determine all values of $\rho_A(i)$ as functions of ρ_A. These values can be used for calculation of the Gibbs adsorption, Γ, defined as

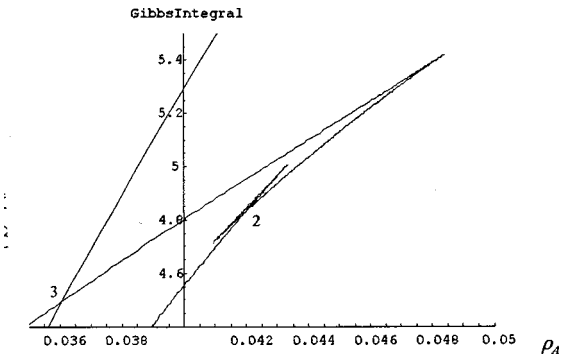

FIG. 7. Fragment of the graph shown in Fig. 6 near the point where $\rho_A\approx 0.042$ and $\sigma/kT\approx 4.8$.

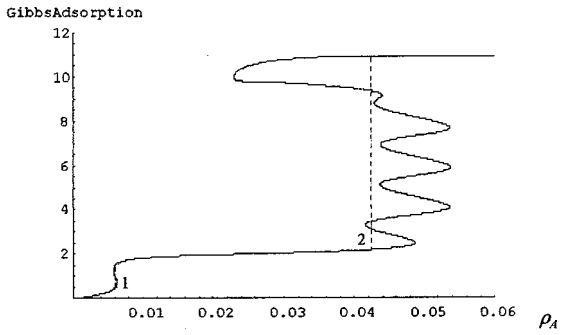

FIG. 8. Isotherm of the Gibbs adsorption in a slitlike pore at $N=12$, $\varepsilon_{AA}/kT=-1.1$, $\varepsilon_{AS}/kT=-3.0$, and $\varepsilon_{AB}/kT=\varepsilon_{BB}/kT=\varepsilon_{BS}/kT=0$.

$$\Gamma=\sum_{i=1}^{N}[\rho_A(i)-\rho_A]. \tag{31}$$

ANALYSIS OF FLUID BETWEEN WALLS

Figure 1 shows the composition of fluid as a function of ρ_A for the cubic lattice and $N=2$ (two symmetric layers). Here, $\varepsilon_{AA}/kT=-1.1$, $\varepsilon_{AS}/kT=-0.9$, $\varepsilon_{AB}/kT=\varepsilon_{BB}/kT=\varepsilon_{BS}/kT=0$, and $\delta=0.0005$. As shown in Fig. 1, $\rho_A(1)$ is multivalued for ranges of ρ_A and ρ_A is multivalued for ranges of $\rho_A(1)$. There is no standard way to find solutions to a mathematical problem when $\rho_A(1)$ is not a function (i.e. is not single valued) of ρ_A and ρ_A is not a function of $\rho_A(1)$. Recently, an algorithm was presented [24] for one equation having a solution like that illustrated in Fig. 1 and this has been used to analyze monolayer adsorption. Here, we extend this algorithm to study multilayer adsorption in slit pores.

Figure 2 shows equilibria for a fluid in a four-layer pore ($N=4$). These calculations are for a cubic lattice with $\varepsilon_{AA}/kT=-1.1$, $\varepsilon_{AS}/kT=-3.0$, $\varepsilon_{AB}/kT=\varepsilon_{BB}/kT=\varepsilon_{BS}/kT=0$, and $\delta=0.0005$. Assuming symmetry in the pore, $\rho_A(1)=\rho_A(4)$, and $\rho_A(2)=\rho_A(3)$. Therefore, only two equations must be solved. Shown in Fig. 2 are $\rho_A(1)$ (left curve) and $\rho_A(2)$ (right curve) as functions of ρ_A. As seen in Fig. 2, $\rho_A(1)$ has two ranges where $\rho_A(1)$ is multivalued with respect to ρ_A; one of these ranges coincides with the range of multivaluedness for $\rho_A(2)$. Figure 3 gives

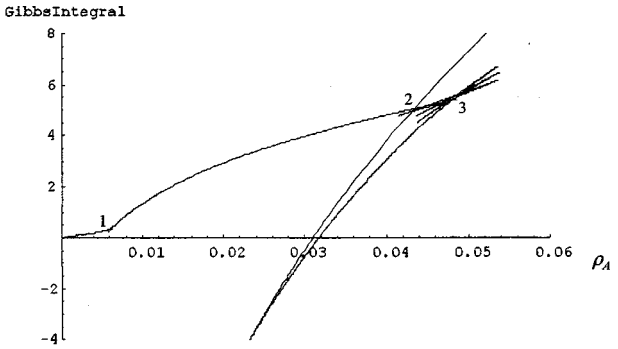

FIG. 9. Gibbs integral as a function of ρ_A for a slitlike pore at $N=12$, $\varepsilon_{AA}/kT=-1.1$, $\varepsilon_{AS}/kT=-3.0$, and $\varepsilon_{AB}/kT=\varepsilon_{BB}/kT=\varepsilon_{BS}/kT=0$. There are three points of self-intersection. However, only two of them are points of binodals.

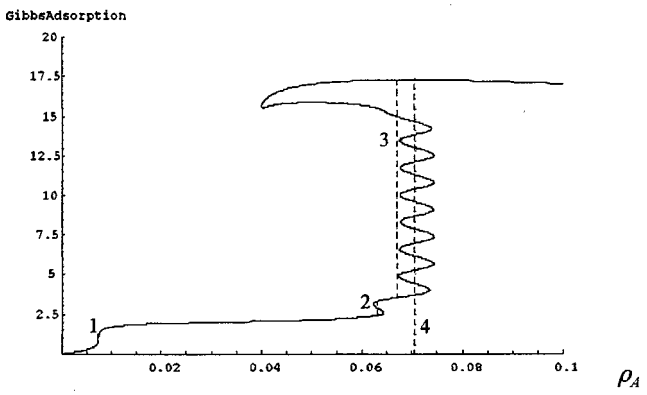

FIG. 10. Isotherm of the Gibbs adsorption in a slitlike pore at $N=20$, $\varepsilon_{AA}/kT=-1.0$, $\varepsilon_{AS}/kT=-3.0$, and $\varepsilon_{AB}/kT=\varepsilon_{BB}/kT=\varepsilon_{BS}/kT=0$.

the isotherm of the Gibbs adsorption for the case shown in Fig. 2. As can be seen from Fig. 3, there are two steps in the isotherm. These are two-dimensional phase transitions; the first step is due to a two-dimensional condensation in the first layer; the second, at a higher concentration, is due to a 2D phase transition in the second layer.

Mathematically, Γ is a multivalued function of ρ_A for the two-dimensional condensations. However, spreading pressures σ in both phases must be equal at equilibrium to maintain mechanical equilibrium. The value of σ can be expressed through the Gibbs integral which for Ono-Kondo model is [19]

$$\frac{\sigma}{kT}=-\int_0^{\rho_A}\frac{\Gamma[1+\rho_A(1-\rho_A)z_0]\Delta}{\rho_A(1-\rho_A)}d\rho_A. \tag{32}$$

Figure 4 gives the Gibbs integral σ/kT as a function of the bulk density ρ_A for $N=4$, $\varepsilon_{AA}/kT=-1.1$, $\varepsilon_{AS}/kT=-3.0$, and $\varepsilon_{AB}/kT=\varepsilon_{BB}/kT=\varepsilon_{BS}/kT=0$. As shown in Fig. 4, there are two points of self-intersection which represent the binodal. These points are indicated in Fig. 3 by dashed lines. At these points, we have two-dimensional condensation.

The point where the three-dimensional condensation occurs can be calculated from the binodal for regular solutions [25]:

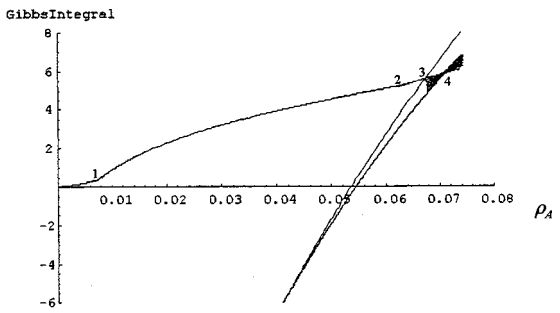

FIG. 11. Gibbs integral as a function of ρ_A for a slitlike pore at $N=20$, $\varepsilon_{AA}/kT=-1.0$, $\varepsilon_{AS}/kT=-3.0$, and $\varepsilon_{AB}/kT=\varepsilon_{BB}/kT=\varepsilon_{BS}/kT=0$. There are four points of self-intersection (1, 2, 3, and 4).

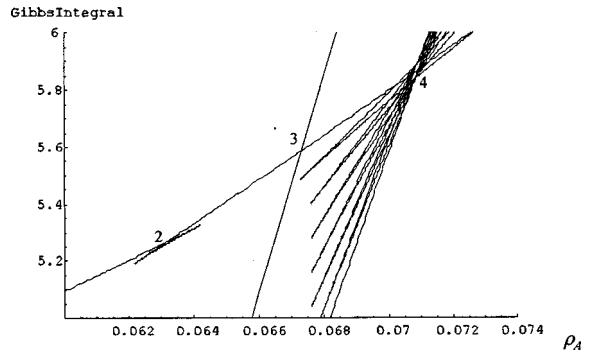

FIG. 12. Fragment of the graph shown in Fig. 11 at smaller scale, with details of self-intersections 2, 3, and 4.

$$\rho_A \exp[(1-\rho_A)^2 z_0 \Delta/2kT] = (1-\rho_A)\exp(\rho_A^2 z_0 \Delta/2kT). \tag{33}$$

For the case shown in Fig. 3, the three-dimensional condensation occurs at $\rho_A \approx 0.0485$. As can be seen from Fig. 3, both two-dimensional phase transitions occur at lower concentrations, i.e., at a density where the bulk is a single phase. It is possible [26] for the 2D transition to lie inside the 3D phase envelope; in such cases, the 2D behavior cannot be observed experimentally.

Figure 5 shows the Gibbs adsorption isotherm in a six-layer slit pore ($N=6$) with the same energies as in Fig. 3. One might expect three steps in this isotherm due to successive condensation in the first, second, and third layers as is observed in isotherms for macroporous adsorbents [22]. However, this does not happen in the case shown in Fig. 5. Rather, one sees that it is ''easier'' to fill both the second and third layers simultaneously than it is to fill the second layer alone. Figure 6 gives the Gibbs integral as a function of ρ_A for this case. Analysis of Fig. 6 shows that there are three self-intersections indicated by numbers of 1, 2, and 3. Self-intersection 2 is not seen well in Fig. 6, therefore in Fig. 7 it is shown with an expanded scale. As shown in Fig. 7, self-intersection 2 occurs in the range of instability around self-intersection 3. Therefore, there are only two binodal points—one for self-intersection 1 and the other for self-intersection 3. Hence, we have only two steps in the adsorption isotherm; these are shown by the two dashed lines. In other words, condensation in the second and in the third layers occurs simultaneously.

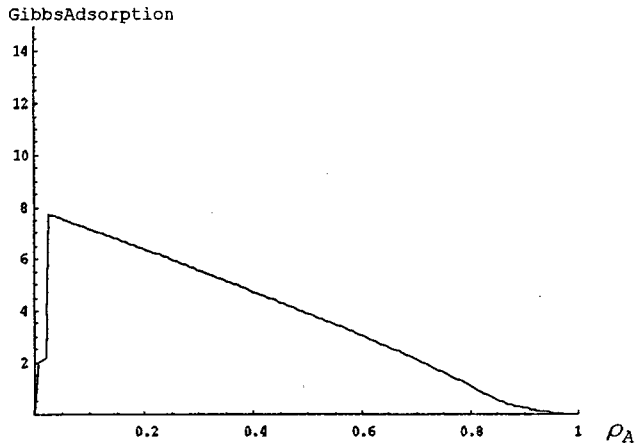

FIG. 13. Isotherm of the Gibbs adsorption for $\varepsilon/kT=-1.4$ and $\varepsilon_s/kT=-4.0$ in eight layer pore calculated by iteration using method of successive substitutions. The calculations indicate that the pore fills at $\rho_A \approx 0.025$.

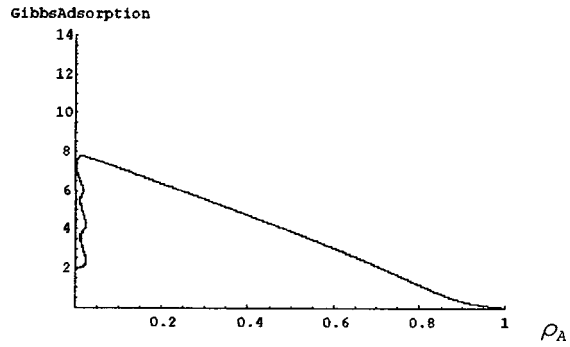

FIG. 14. Isotherm of the Gibbs adsorption for $\varepsilon/kT=-1.4$ and $\varepsilon_s/kT=-4.0$ in eight layer pore calculated by new procedure. This method shows that the pore virtually fills at $\rho_A \approx 0.014$.

Figure 8 shows the isotherm of the Gibbs adsorption in a slitlike, 12-layer pore for $\varepsilon_{AA}/kT=-1.1$, $\varepsilon_{AS}/kT=-3.0$, and $\varepsilon_{AB}/kT=\varepsilon_{BB}/kT=\varepsilon_{BS}/kT=0$. The Gibbs integral for this case is shown in Fig. 9. As can be seen from Fig. 9, there are three points of self-intersection (1, 2, and 3). However, point 3 is in the region of instability; therefore, there are only two steps in the adsorption isotherm shown in Fig. 8. These two steps translate into self-intersections 1 and 2 in Fig. 9. Therefore, in 12-layer pore, at these conditions, an increase of ρ_A results in the two-dimensional condensation in the two surface layers, and further increase of ρ_A leads to the condensation in all other layers simultaneously. This analysis sheds new light on the concept of volume filling of micropores as described by Polanyi [27] and Dubinin and coworkers [28,29].

Figure 10 shows the Gibbs adsorption isotherm in a slitlike pore at $N=20$, for $\varepsilon_{AA}/kT=-1.0$, $\varepsilon_{AS}/kT=-3.0$, and $\varepsilon_{AB}/kT=\varepsilon_{BB}/kT=\varepsilon_{BS}/kT=0$. The Gibbs integral as a function of ρ_A is given in Fig. 11 with four points of self-intersection. A more detailed picture of self-intersections 2, 3, and 4 is shown in Fig. 12. So, step 1 in Fig. 10 corresponds to self-intersection 1 in Figs. 11 and 12. This step is the two-dimensional phase transition in the first (surface) layer. Step 2 in Fig. 10 translates into self-intersection 2 in Figs. 11 and 12. This is a two-dimensional phase transition

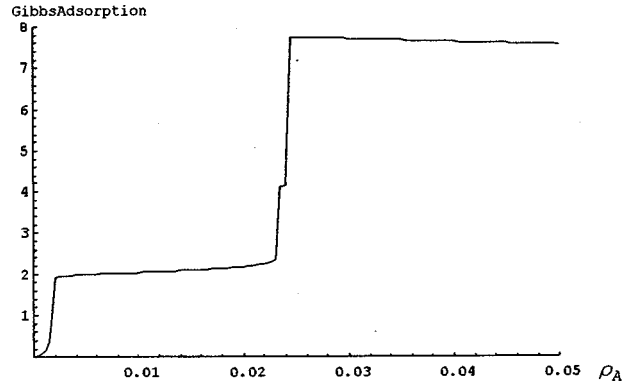

FIG. 15. Fragment of Fig. 13 in a smaller scale.

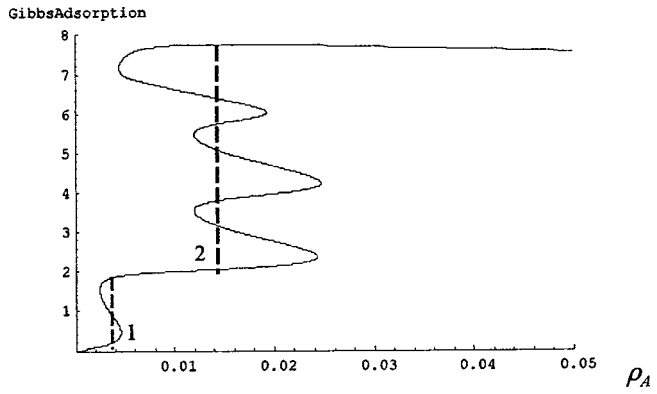

FIG. 16. Fragment of Fig. 14 in a smaller scale.

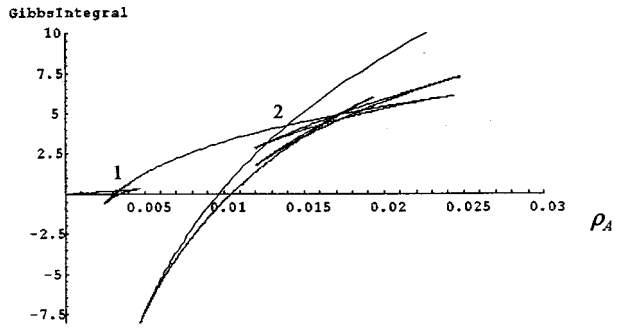

FIG. 17. Gibbs integral for the case shown in Fig. 16.

in the second layer. Step 3 in Fig. 10 is condensation of all other layers; this step corresponds to self-intersection 3 in Figs. 11 and 12. Finally, the dotted line 4 in Fig. 10 corresponds to the bunch of self-intersections denoted by No. 4 in Figs. 11 and 12. At this point, the value of $\rho_A \approx 0.0705$ is the binodal point of three-dimensional phase transition for $\varepsilon_{AA}/kT = -1.0$, and $\varepsilon_{AB}/kT = \varepsilon_{BB}/kT = \varepsilon_{BS}/kT = 0$. This value of ρ_A is the solution of Eq. (33). So, the dotted line 4 in Fig. 10 indicates the three-dimensional condensation in nonconfined space.

As shown in Fig. 10, condensation of adsorbate in the pore occurs at the density lower than that in nonconfined space. This difference is about 5% for 20 layer pore. For lower N, this difference becomes greater; for $N=12$, the difference in ρ_A between points 2 and 3 in Fig. 9 is about 10%. Our calculations show that this difference vanishes as the distance between walls increases.

COMPARISON WITH THE METHOD OF ITERATIONS AND NEW INFORMATION ON PHYSICAL MECHANISM OF CAPILLARY CONDENSATION

Figure 13 and 14 compare the isotherm of the Gibbs adsorption for an eight-layer pore at $\varepsilon/kT = -1.4$ and $\varepsilon_s/kT = -4.0$ calculated in two different ways. In Fig. 13, the adsorption isotherm is calculated by iteration using the method of successive substitutions. In Fig. 14, the adsorption isotherm is calculated by the new method described in this paper. In Figs. 15 and 16 the ranges of phase transitions are shown with an expanded scale. As shown in Fig. 15, the first step occurs at $\rho_A \approx 0.002$, and the second step (seen in Fig. 15 as a double step) occurs at $\rho_A \approx 0.024$. Figure 17 gives the Gibbs integral where self-intersections indicate points in binodal and steps in the isotherm. As shown in Figs. 16 and 17, there are two steps, at $\rho_A \approx 0.0035$ and at $\rho_A \approx 0.0145$. Hence, the method of successive substitutions gives dramatically different results. It predicts the first step in the isotherm occurs at a density that is too low (by 50%) and the second step in the isotherm at a density that is too high (by 70%). It also incorrectly predicts three steps where there are only two. Hence, it gives incorrect predictions for both wetting phase transitions and capillary condensation.

Of course, it is possible to adjust the method of iteration and multiple initial guesses to map the regions where there are multiple solutions. Lastoskie, Gubbins, and Quirke [30] recognized that there may be multiple solutions, but did not focus on the details of the numerical calculations. They also performed Gibbs ensemble simulations [31] and demonstrated agreement with DFT results. The results presented here show that the method of solution greatly affects the predicted behavior of confined fluids. Hence, it is important to have a numerical algorithm that gives multiple solutions in the range of phase transitions. The method proposed in this paper enables such calculations for lattice DFT. It also should be applicable to off-lattice DFT.

The advantage of this algorithm is that it gives the entire curve where the grand potential (or free energy) is minimum, including all binodal and spinodal points; we are not aware of other numerical method that can give these details. However, such information is important because it shows the physical mechanisms responsible for capillary condensation. In particular, simultaneous condensation in the second and third layers shown in Fig. 5 is possible because point 2 in Figs. 6 and 7 (the binodal point for condensation in the second layer) is at a higher concentration than self-intersection 3 (the binodal point for condensation in the third layer). This occurs because there is a synergism between the walls that, in effect, makes it easier to fill the third layer than to fill the second layer. In this example, point 2 is ''hidden'' but important. Analysis of this hidden point 2 can predict when condensation in the second layer and condensation in the third layer become independent and give separate steps in the isotherm.

In the example given in Figs. 10–12, point 3 is independent of point 2, and they translate into separate steps in the isotherm. However, point 4, which is the binodal point of the three-dimensional condensation, is in the range of instability around point 3, the binodal point of condensation in the third layer. Therefore, capillary condensation occurs before the condensation in the bulk. However, by changing energies and the pore width, point 4 can split and give rise to another independent step, and so on. This new method is able to give new insights in the problem of capillary condensation, and, more generally, in the physics of confined fluids.

[1] B. V. Deriagin, Acta Physicochim. URSS **12**, 181 (1940).
[2] W. F. Saam, and M. W. Cole, Phys. Rev. B **11**, 1086 (1975).
[3] R. Evans, U. M. B. Marconi, and P. Tarazona, J. Chem. Phys. **84**, 2376 (1986).
[4] S. Dietrich, in *Phase Transitions and Critical Phenomena*, edited by C. Domb and J. L. Lebowitz (Academic, London, 1988), Vol. 12, p. 1.
[5] R. F. Cracknell, D. Nicholson, and N. Quirke, J. Chem. Soc., Faraday Trans. **90**, 1487 (1994).
[6] G. B. Hess, M. J. Sabatini, and M. H. W. Chan, Phys. Rev. Lett. **78**, 1739 (1997).
[7] M. J. Bojan, and W. A. Steele, Carbon **36**, 1417 (1998).
[8] S. M. Gatica, M. M. Calbi, and M. W. Cole, Phys. Rev. E **59**, 4484 (1999).
[9] E. Cheng, M. W. Cole, W. F. Saam, and J. Treiner, Phys. Rev. B **46**, 13 967 (1992).
[10] J. Walton and N. Quirke, Mol. Simul. **2**, 361 (1989); E. Cheng, M. R. Swift, and M. W. Cole, J. Chem. Phys. **99**, 4064 (1993).
[11] L. D. Gelb and K. E. Gubbins, Phys. Rev. E **55**, R1290 (1997); **56**, 3185 (1997).
[12] M. W. Maddox, C. M. Lastoskie, N. Quirke, and K. E. Gubbins, in *Fundamentals of Adsorption*, edited by M. D. LeVan (Kluwer, Boston, 1996), p. 571.
[13] R. Radhakrishnan, and K. E. Gubbins, Phys. Rev. Lett. **79**, 2847 (1997).
[14] P. Tarazona, Phys. Rev. A **31**, 2672 (1985).
[15] P. Tarazona, Mol. Phys. **60**, 573 (1987).
[16] M. Sliwinska-Bartkowiak, S. L. Sowers, and K. E. Gubbins, Langmuir **13**, 1182 (1997).
[17] B. Carnahan, and J. O. Wilkes, *Digital Computing and Numerical Methods* (Wiley, New York, 1973), p. 368; G. A. Korn and T. M. Korn, *Mathematical Handbook for Scientists and Engineers* (McGraw-Hill, New York, 1961), Sect. 20.2.
[18] N. A. Modine, G. Zumbach, and E. Kaxiras, Phys. Rev. B **55**, 10 289 (1997).
[19] S. Ono and S. Kondo, *Molecular Theory of Surface Tension in Liquids*, in *Encyclopedia of Physics*, edited by S. Flügge (Springer, Berlin, 1960), Vol. 10, p. 134.
[20] J. S. Rowlinson, and B. Widom, *Molecular Theory of Capillarity* (Clarendon, Oxford, 1982); J. E. Lane, and C. H. J. Johnson, Aust. J. Chem. **20**, 611 (1967).
[21] J. E. Lane, Aust. J. Chem. **21**, 827 (1968); A. R. Altenberger, and J. Stecki, Chem. Phys. Lett. **5**, 29 (1970).
[22] G. L. Aranovich, and M. D. Donohue, J. Chem. Phys. **104**, 3851 (1996); G. L. Aranovich, M. D. Donohue, J. Colloid Interface Sci. **200**, 273 (1998).
[23] G. A. Korn and T. M. Korn, *Mathematical Handbook for Scientists and Engineers* (McGraw-Hill, New York, 1961), Sect. 11.3.
[24] G. L. Aranovich and M. D. Donohue, Computers Chemistry **22**, 429 (1998).
[25] J. M. Prausnitz, *Molecular Thermodynamics of Fluid-Phase Equilibria* (Prentice Hall, Englewood Cliffs, NJ, 1969).
[26] T. Hocker, G. L. Aranovich, and M. D. Donohue, J. Colloid Interface Sci. **211**, 61 (1999).
[27] M. Polanyi, Verh. Dtsch. Phys. Ges. **16**, 1012 (1914); Trans. Faraday Soc. **28**, 316 (1932).
[28] M. M. Dubinin and L. V. Radushkevich, Dokl. Akad. Nauk SSSR **55**, 327 (1947); M. M. Dubinin and E. D. Zaverina, Zh. Fiz. Khim. **23**, 1129 (1949).
[29] S. J. Gregg and K. S. W. Sing, *Adsorption, Surface Area and Porosity* (Academic, New York, 1982), Sect. 4.4.
[30] C. Lastoskie, K. E. Gubbins, and N. Quirke, J. Phys. Chem. **97**, 4786 (1993).
[31] C. Lastoskie, K. E. Gubbins, and N. Quirke, Langmuir **9**, 2693 (1993).